

BIOCHE 01533

## Intramolecular excimer formation of pyrene-labeled lipids in lamellar and inverted hexagonal phases of lipid mixtures containing unsaturated phosphatidylethanolamine

Kwan Hon Cheng <sup>a</sup>, Sun-Yung Chen <sup>a</sup>, Peter Butko <sup>a</sup>, B. Wieb Van Der Meer <sup>b</sup>  
and Pentti Somerharju <sup>c</sup>

<sup>a</sup> Department of Physics, Texas Tech University, Lubbock, TX 79409, <sup>b</sup> Department of Physics and Astronomy, Western Kentucky University, Bowling Green, KY 42101, U.S.A. and <sup>c</sup> Department of Medical Chemistry, Helsinki University, Finland

Received 28 June 1990

Revised manuscript received 22 August 1990

Accepted 23 August 1990

Intramolecular excimer formation; Lipid non-bilayer phase; Phase transition; Fluorescence spectroscopy; Phosphatidylethanolamine; Diacylglycerol

The rates of intramolecular excimer formation of di(1'-pyrenemyristoyl)phosphatidylcholine (dipyPC) in dioleoylphosphatidylethanolamine (DOPE), egg PE/diolein (DG) and dilinoleoyl-PE (DLPE)/1-palmitoyl-2-oleoyl-PC (POPC) were studied at different temperatures and lipid compositions. Both the excimer-to-monomer intensity ratio and the excimer association rate constant were employed to quantify the rate of excimer formation. The latter was calculated from the measured monomer fluorescence lifetime of dipyPC. We observed that the rate of excimer formation was sensitive to either the temperature-induced or lipid composition-induced lamellar-to-inverted hexagonal phase transition of the above lipid systems. As the lipids entered the inverted hexagonal phase, the rate of excimer formation increased at the temperature-induced phase transition for DOPE, but decreased at the composition-induced phase transition for both TPE/DG and DLPE/POPC systems by increasing the DG% and decreasing the PC%, respectively. We conclude that the rate of intramolecular excimer formation of dipyPC in the non-lamellar phase is influenced both by the intra-lipid free volume of the hydrocarbon region and the intra-rotational dynamics of the two lipid acyl chains.

### 1. Introduction

Excimer-forming fluorophores, such as free pyrene and pyrene-labeled lipid analog, are widely employed for studying the physical state of lipid bilayers [1–4]. By measuring the rate of excimer formation of these fluorophores, molecular information pertaining to the diffusional behavior of lipids in different lamellar phases, e.g., gel and liquid crystalline, has been determined [1–4]. Recently, this excimer-formation technique has also

been applied to studying the non-lamellar phase (inverted hexagonal phase) of unsaturated phosphatidylethanolamine (PE) and other binary lipid mixtures containing PE [5].

The basic principle governing the excimer formation among fluorophores is the association of a fluorophore in its first excited singlet state with another non-excited fluorophore [6]. It is well established that the excimer formation of free pyrene or single pyrene-labeled lipid fluorophores in lipid membranes is an intermolecular collisional event occurring inside the membrane hydrocarbon region [3,4]. As a diffusional-control process, the rate of excimer formation depends on the concentration of the fluorophores, the motional order

Correspondence address: K.H. Cheng, Biophysics Laboratory, Department of Physics, Texas Tech University, Lubbock, TX 79409, U.S.A.

of the host lipids and the inter-lipid free volume of the membrane. An inherent assumption of a uniform distribution of the fluorophores among the lipid matrix is also required. In contrast, the excimer formation of two fluorophores that are attached to the same molecule refers to an intramolecular collisional event. The rate of this intramolecular excimer formation event depends on the intra-rotational dynamics and local geometry of the parent molecule which contains the two excimer-forming fluorophores. Moreover, the rate is independent of the concentration of fluorophores at sufficiently low fluorophore/lipid ratio [7–9]. Numerous applications of this intramolecular excimer formation technique in lipid studies have been initiated. Among which, linear chain (such as bis(4-biphenylmethyl) ether [7,8]) and lipid analog [9] probes were used to study the physical state of lipid lamellar phases.

This study represents an initial attempt to investigate the physical state of lipid non-lamellar phases using the intra-molecular excimer formation technique. A lipid analog, di(1'-pyrenemyristoyl)phosphatidylcholine (dipyPC), was employed as an intramolecular excimer-forming lipid probe. Various lipid systems, dioleoylphosphatidylethanolamine (DOPE), egg PE/diolein and dilinoleoyl-PE/1-palmitoyl-2-oleoyl PC, were used in this study. These lipid systems have previously been shown to exhibit lamellar to non-lamellar phase transitions at defined temperatures and lipid compositions [10–13].

## 2. Materials and methods

Dioleoylphosphatidylethanolamine (DOPE), dioleoylphosphatidylcholine (DOPC), 1,2-dioleoyl-*sn*-glycerol (diolein), PE transphosphatidylated from egg PC (TPE), dilinoleoyl-PE (DLPE), and 1-palmitoyl-2-oleoylphosphatidylcholine (POPC) in chloroform were purchased from Avanti Polar Lipids (Birmingham, AL). These lipids were used without further purification. No detectable fluorescence signals were found in the lipids. The intramolecular excimer forming fluorophore, di(1'-pyrenemyristoyl)-PC (dipyPC), was synthesized by methods described previously [14]. The

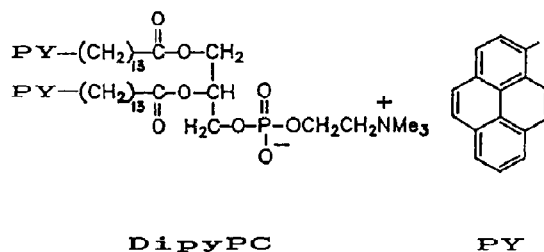


Fig. 1. Chemical structure of dipyPC.

chemical structure of a dipyPC molecule is shown in Fig. 1. The two pyrene (PY) molecules are separately attached to the terminal methyl ends of the two myristic acyl chains of a PC lipid. The fluorophores and lipids were mixed in chloroform at a molar ratio of 0.001. The mixture was then dried under nitrogen in a clean pyrex tube and further kept under vacuum for more than 5 h to ensure complete removal of organic solvent. The thin lipid film formed on the tube was hydrated in an aqueous buffer (100 mM NaCl, 10 mM Tes, 2 mM EDTA; pH 7.4) at 0°C. The suspension was vortexed rigorously and under mild sonication for a few seconds. Thereafter, the mixture was incubated at 0°C for about 20 h in the dark to ensure proper hydration. Upon further dilution to approx. 100 µg/ml, the sample was put into a 10 mm quartz cuvette. The sample temperature was regulated by an external water-jet circulator connected to a thermostated cell. The temperature of the sample was directly determined by inserting a microtip thermistor probe (YSI-427) into the cuvette at approx. 5 mm above the light path and recorded by a digital thermometer (VWR 500).

An ISS multifrequency cross-correlation fluorometer (Urbana, IL) was used for all the fluorescence spectra and lifetime measurements. The excitation source was an He-Cd laser (Liconix 4240NB) which possesses an output of 17 mW at 325 nm.

For the fluorescence spectral measurements, excitation and emission slit widths were set at 4 nm. Scattering contributions, which were determined from samples prepared under identical preparative and measuring procedures but in the absence of fluorophores, were subtracted from the fluorescence signals. This procedure yielded corrections

similar to those following the method of Eisinger et al. [15] (differences less than 5%). The value of the steady-state excimer to monomer intensity ratio was calculated from the fluorescence intensities at 485 and 390 nm, respectively.

For the fluorescence lifetime measurements, fluorescence signals at 390 nm were determined and compared with a reference, 1,4-bis[2-(5-phenyloxazolyl)]benzene (POPOP) in methanol [16]. The fluorescence lifetime of POPOP is 1.34 ns. The values of demodulation ratio and phase delay were measured as a function of modulation frequency between 0.1 and 10 MHz. The frequency-domain data were fitted by a double-exponential intensity decay function.

$$I(t) = \alpha_1 e^{-t/\tau_1} + \alpha_2 e^{-t/\tau_2} \quad (1)$$

where the short component was fixed at  $\tau_1 = 5$  ps in order to account for the light scattering. Here,  $\alpha_1$  and  $\alpha_2$  are the pre-exponential factors. Since the demodulation ratio is less sensitive to scattering than the phase delay, almost identical results were obtained by fitting the demodulation data with a single-exponential function.

The monomer lifetime  $\tau$  of pyrene is related to the excimer formation rate constant  $K$  by the expression,

$$\begin{aligned} \tau^{-1} &= K_r + K_{nr} + K \\ &= \tau_0^{-1} + K \end{aligned} \quad (2)$$

where  $K_r$  and  $K_{nr}$  are the radiative and non-radiative decay rate constants, respectively, and  $\tau_0$  the monomer lifetime of pyrene in the absence of excimer formation. Note that the above equation is valid only under the assumption that the excimer dissociation rate constant is much smaller than  $K$ .

In the study of the temperature dependence of  $K$ , the values of  $\tau$  were determined for temperatures varying from 0 to 40°C. It has been shown [17] that  $\tau_0$  of pyrene in the lipid hydrocarbon region has an intrinsic temperature-dependent behavior. This temperature dependence can be described by a linear equation,  $\tau_0 = 200 - 1.5T$ , according to the published data [17].  $\tau_0$  is expressed in units of ns and  $T$  is the temperature in degree celsius.

### 3. Results

Excimer-to-monomer ( $E/M$ ) intensity ratios for dipyPC in DOPE and DOPC were measured at different temperatures (0–40°C). As shown in fig. 2A, the  $E/M$  ratio for DOPE was around 0.5 at 0°C, and increased slightly with temperature

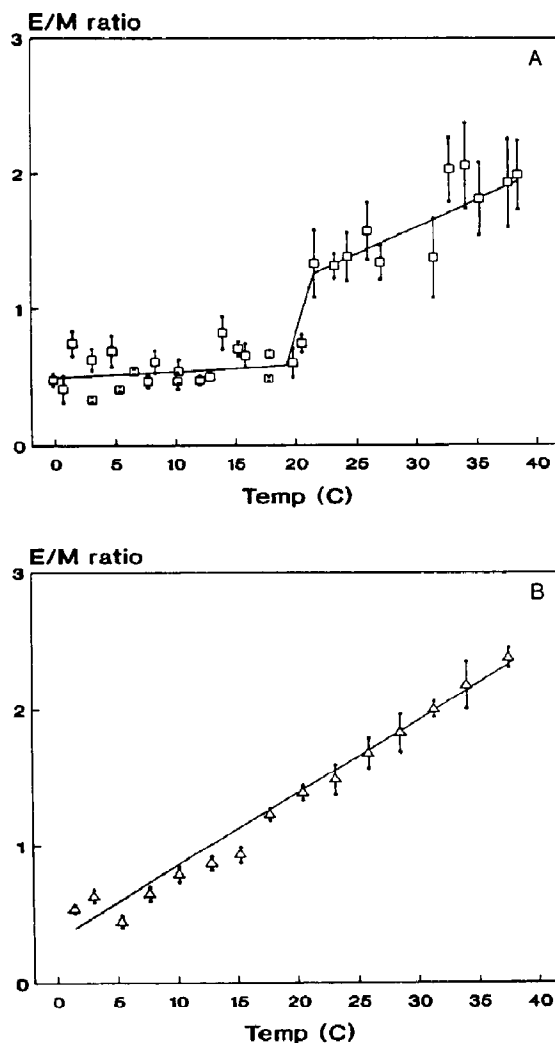


Fig. 2.  $E/M$  ratio of dipyPC in DOPE (A) and DOPC (B) vs temperature. Molar ratio of dipyPC/lipid, 0.001; excitation wavelength, 325 nm. The  $E/M$  ratio was calculated from the ratio of fluorescence intensities at 485 and 390 nm, respectively, at each temperature. The error bars represent the standard errors of measurements.

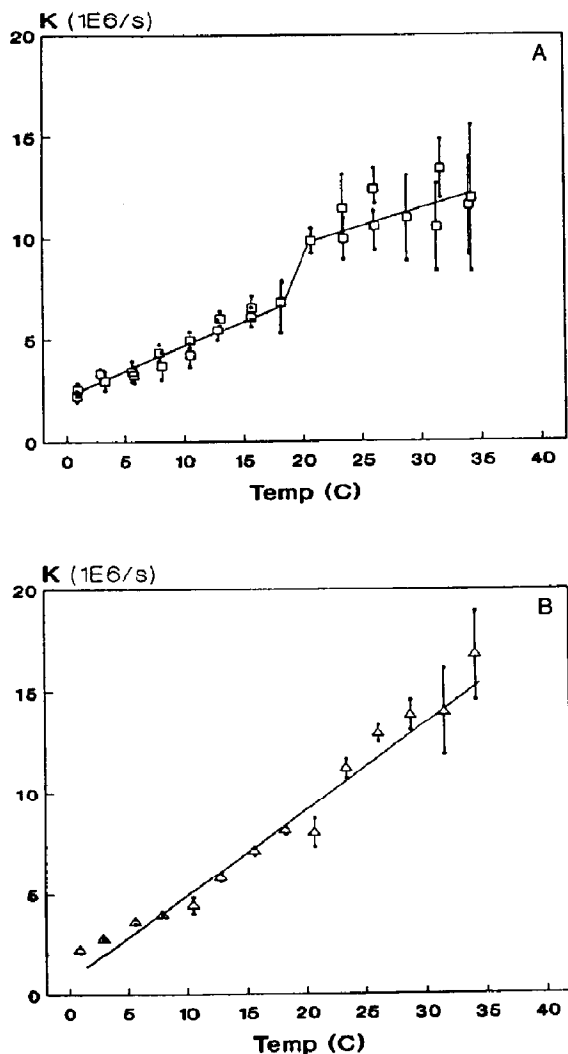


Fig. 3.  $K$  of dipyPC in DOPE (A) and DOPC (B) vs temperature. The values of  $K$  were calculated from the monomer fluorescence lifetime of dipyPC (see section 2). Excitation, 325 nm; fluorescence, measured at 390 nm. The error bars represent the standard errors of measurements.

from 0 to 20  $^{\circ}C$ . Thereafter, the  $E/M$  ratio increased abruptly by almost 3-fold at 22  $^{\circ}C$ . At higher temperatures, a linear increase in  $E/M$  ratio with temperature was observed. The slope of  $E/M$  ratio vs temperature for the high-temperature region (20–40  $^{\circ}C$ ) was higher than that for the lower temperature region (0–20  $^{\circ}C$ ). Similar meas-

urements on  $E/M$  ratios were performed for dipyPC in DOPC as shown in fig. 2B. A linear increase in the  $E/M$  ratio with temperature was found. No abrupt increase in the  $E/M$  ratio was observed.

The monomer lifetimes of dipyPC at 390 nm were measured using the phase-modulation technique at different temperatures. The corresponding association rate constants  $K$  were subsequently determined (see eq. 2) and shown in fig. 3A. Similar to the results for the  $E/M$  ratios, an abrupt increase in  $K$  was seen at approx. 17  $^{\circ}C$  for DOPE. However, the value of  $K$  at 17  $^{\circ}C$  was only about 50% higher than that at lower temperatures. A linear dependence of  $K$  on temperature was found for DOPC as shown in fig. 3B. Also, no abrupt increase in the value of  $K$  was observed.

Measurements of  $E/M$  ratio and  $K$  were performed for dipyPC in binary lipid mixtures con-

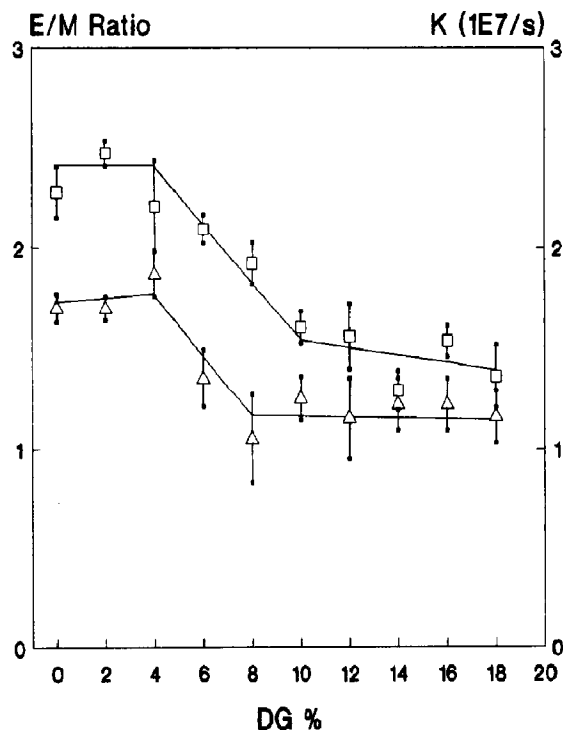


Fig. 4.  $E/M$  ratio ( $\square$ ) and  $K$  ( $\triangle$ ) of dipyPC in TPE/DG binary mixtures as a function of DG% at 23  $^{\circ}C$ . The error bars represent the standard errors of measurements.

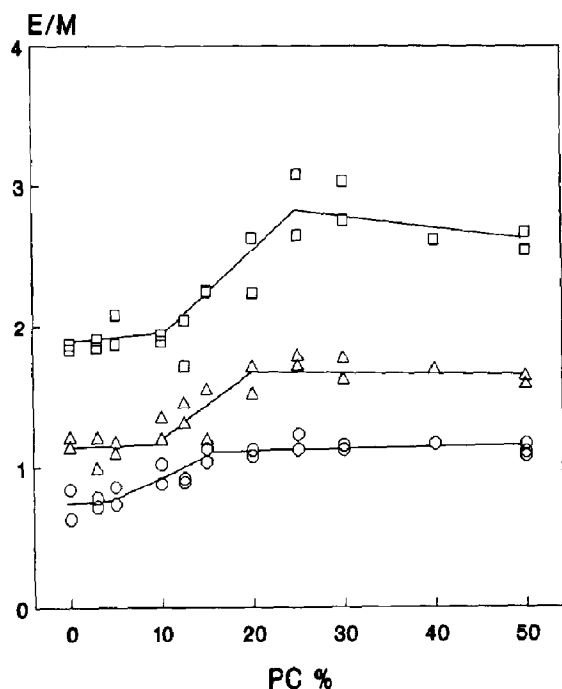


Fig. 5.  $E/M$  ratio of dipyPC in DLPE/POPC binary mixtures as a function of PC%. Temperature: 5 (○), 15 (Δ) and 30°C (□). Data from two independently prepared samples are shown.

taining different ratios of TPE and diolein (DG) at 23°C as shown in fig. 4. A sigmoidal behavior with breakpoints at approx. 4 and 8% DG was observed for either  $E/M$  ratio or  $K$  vs DG% curves. The values of  $E/M$  ratio or  $K$  at high DG content (8–18%) were about 50% less than that at low DG content (0–4%).

Using another binary lipid mixture consisting of POPC and DLPE, the  $E/M$  ratios of dipyPC were measured as a function of PC content and at three different temperatures (5, 15 and 30°C) as shown in fig. 5. These PE/PC lipid samples, especially those with low PC contents, tended to aggregate at long incubation times. The lifetime measurements of dipyPC were therefore not performed for these lipid mixtures. In general, the  $E/M$  ratio increased with temperature for all PC contents (0–50% PC). At 5°C, the  $E/M$  ratio was approx. 0.8 as PC varied from 0 to 5%. It increased slightly to 1.0 as the PC content increased further from 5 to 15%. Thereafter, it remained

constant for PC > 15%. As the temperature increased to 15°C, the  $E/M$  ratio started at 1.2 and ended at 1.8. The transitions occurred at 10 and 20% PC. At a higher temperature (30°C), a similar trend was also observed. Yet the transitions were at 10% and 25% PC. In addition, the  $E/M$  ratio for PC > 25% was almost 50% higher than that for PC < 10%. Assuming that the intramolecular ex-

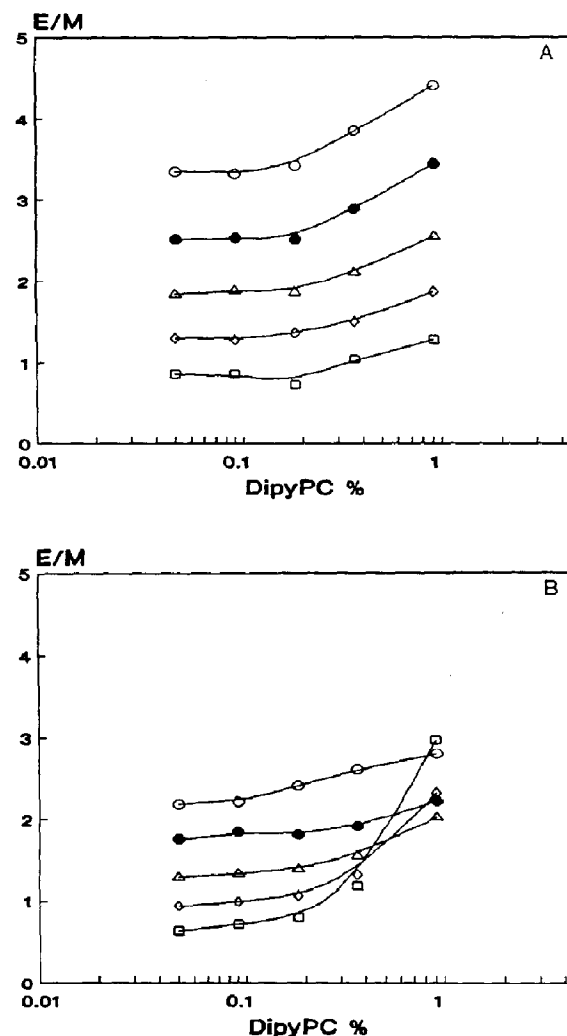


Fig. 6.  $E/M$  ratio of dipyPC in DLPE/POPC binary mixtures as a function of dipyPC% (dipyPC vs total lipid) for 50% PC (A) and 3% PC (B). Temperature: 0 (□), 10 (◇), 20 (Δ), 30 (●) and 40°C (○).

cimer formation of dipyPC obeys a simple two-state process, the activation energy of this process can be estimated from the Arrhenius plots of  $E/M$  ratios (results not shown). The activation energies were found to be approx. 6.9 and 6.2 kcal/mol for 0 and 50% DOPC, respectively.

The dependence of  $E/M$  ratio on dipyPC concentration for 3 and 50% DOPC at different temperatures (0, 10, 20, 30 and 40°C) is illustrated in fig. 6. The  $E/M$  ratios of dipyPC in either 3 or 50% DOPC were found to be constant (i.e., independent of dipyPC%) for dipyPC concentrations less than 0.2% at all temperatures. For dipyPC higher than 0.2%, the  $E/M$  ratio started to increase linearly with concentration. Note that the concentration of dipyPC (0.1%) employed in this study was obviously within the plateau regions of all the  $E/M$  ratio vs probe concentration curves. As shown in fig. 6B, for 3% DOPC, abrupt increases in the  $E/M$  ratio with increasing probe concentration occurred at low temperatures (0–10°C) and high dipyPC contents (> 0.2%). A tendency for some of the dipyPC probes to phase separate from the host lipid mixtures was suspected at those low temperatures.

#### 4. Discussion

A new observation of this study is that the rate of intramolecular excimer formation of dipyPC is rather sensitive to the lamellar-to-non-lamellar phase transition of unsaturated PE and binary lipid mixtures of PE/DG and PE/PC. Note that the present technique of intramolecular excimer formation of pyrene-labeled probes has previously been applied to membrane phase transitions. Yet those transitions were confined to lamellar phase transitions exclusively, e.g., pretransitions and gel-to-liquid crystalline transitions of lipids [1,4,7–9].

In the temperature study of DOPE, an abrupt increase in the value of the  $E/M$  ratio or  $K$  of dipyPC occurs at approx. 17–20°C. A previous time-resolved fluorescence depolarization study on DOPE [18] which employed an identical sample preparation procedure to that in this study has been performed. In that study, a fluorescent lipid, 2-[3-(diphenylhexatrienyl)propanoyl]-3-palmitoyl-

L- $\alpha$ -phosphatidylcholine (DPH-PC) was used. Obviously, the fluorescence study on DPH-PC provides the molecular information on the intermolecular interactions among the lipids, while this study focuses on the intramolecular interactions of the two fatty acyl chains within a single lipid. From the DPH-PC study, both the calculated order parameter and the rotational diffusion constant declined abruptly at around 12°C; and the transition is quite broad, i.e., starting at approx. 10°C and ending at about 18°C. Therefore, the transition temperature depicted by the present dipyPC study conforms only with the completion temperature of the lamellar-to-inverted hexagonal phase transition of DOPE. It is further concluded that dipyPC may preferentially partition into the lamellar phase in the temperature region (10–18°C) at which both lamellar and inverted hexagonal phases co-exist.

The intramolecular excimer formation behavior of dipyPC in TPE/DG lipid mixtures which exhibit a lamellar-to-inverted hexagonal phase transition was investigated. Instead of using temperature to change the lipid phase, the lamellar-to-inverted hexagonal transition is achieved by varying the composition of the lipid mixture. A previous X-ray diffraction study [11] has established that the lamellar to inverted hexagonal phase transition occurs at around 4% DG. Between 4 and 7% DG, co-existing lamellar and inverted hexagonal phases are evident. For higher DG%, the lipid mixtures are predominantly in the inverted hexagonal phase. A recent Fourier transform infrared study on this TPE/DG system further confirms the above structural phase assignments (manuscript in preparation). In our present fluorescence study, abrupt declines in the values of  $E/M$  and  $K$  occur at similar phase boundaries. These results suggest that the rate of intramolecular excimer formation declines as the lipids change to hexagonal phase upon altering the compositions of the lipid mixtures.

There are two distinctive differences between the temperature-induced and composition-induced lamellar-to-inverted-hexagonal phase transitions. First, the composition study reveals both the starting and ending points for the inverted-hexagonal phase. Yet the temperature study reveals only the

ending point. Second, the intramolecular excimer formation rate in the lamellar phase is higher than that in the inverted-hexagonal phase for the composition study whereas an opposite trend is evident for the temperature study. The first difference may be related to the differential solubility or miscibility behavior of dipyPC in lamellar vs inverted-hexagonal phase. The second difference can be explained by the differential geometrical and dynamical influences of the lipid fatty acyl chains on the intramolecular excimer formation. At a given temperature, the two pyrene molecules of a dipyPC probe may exist in different conformations due to the presence of various gauche rotamers along the fatty acyl chains and to the intrinsic geometry of the dipyPC molecule. Among various conformational states of the fluorophore, only one particular conformation leads to excimer formation. This distinct conformation refers to the state in which the two pyrene molecules are in direct contact and in perfect orientational alignment [6]. The number of different conformational states and the rate of transition from one to the other are strongly dependent upon the physical state of the host lipids. The former is influenced by the local geometry or intra-lipid free volume while the latter by the intra-rotational dynamics of the lipid chains. With this concept in mind, the phenomenon that the rate of excimer formation increases with temperature at the lamellar-to-inverted hexagonal phase transition can be visualized as an enhancement of rate of transition among different conformers of the probe. On the other hand, the decrease in the rate of excimer formation with composition (DG%) at the phase transition suggests that the number of conformational states increases with DG content. This appears to conform with the molecular model proposed by Gruner and co-workers [10] on lipid non-lamellar phases. Within the context of this model, the lipid chains occupy more intra-lipid free volume in the inverted-hexagonal phase than that in the lamellar phase, particularly near the terminal methyl ends of the fatty acyl chains. Consequently, this model can also be interpreted as an increase in the number of conformational states of the fluorophore due to the cylindrical packing geometry of the lipids.

Binary POPC/DLPE lipid mixtures which exhibit lamellar and non-lamellar phases were also investigated. Previous  $^{31}\text{P}$ -NMR, X-ray diffraction, electron microscopy, and time-resolved fluorescence measurements [12,13] on these lipid mixtures revealed the existence of three distinct zones. They are lamellar (20% PC and higher), intermediate (5–20% PC) and inverted hexagonal phases (0–5% PC). Based upon the above phase boundary description, it is concluded that the  $E/M$  ratio of dipyPC drops abruptly from the lamellar to intermediate phase and starts to level off as the lipids enter the inverted hexagonal phase. Based on the  $^{31}\text{P}$ -NMR and electron microscopy studies [13], the phase boundary between the intermediate and lamellar phases has a slight temperature dependence. Essentially, this phase boundary shifts toward higher PC% as the temperature increases. Interestingly, the break points at which the changes occur in the  $E/M$  ratio agree with the above phase boundary description. Our fluorescence result suggests that substantial changes in the intra-lipid free volume occur as the lipids enter from the lamellar phase to the intermediate phase. The intermediate phase has been hypothesized to be made up of disordered amorphous, cubic and lamellar/inverted-hexagonal co-existing phases [13]. The present study indicates that the intra-lipid free volume in the intermediate phase is greater than that in the lamellar phase, while the hexagonal phase has the greatest free volume among the lamellar and intermediate phases.

### Acknowledgements

This work was supported by grants from the National Cancer Institute (PHS CA 47610) and the Robert A. Welch Research Foundation (D-1158) to K.H.C. B.W.V. acknowledges support from the National Science Foundation and the Kentucky EPSCoR program (RII-8610671).

### References

- 1 H.J. Galla and J. Luisetti, *Biochim. Biophys. Acta* 596 (1980) 108.

- 2 R.C. Heresko, I.P. Sugar, Y. Barenholz and T.E. Thompson, *Biochemistry* 25 (1986) 3813.
- 3 M.D. King and D. Marsh, *Biochim. Biophys. Acta* 862 (1986) 231.
- 4 J. Eisinger, J. Flores and W.P. Petersen, *Biophys. J.* 49 (1986) 987.
- 5 S.Y. Chen, K.H. Cheng and D.M. Ortalano, *Chem. Phys. Lipids* 53 (1990) 321.
- 6 J.B. Birk, *Photophysics of aromatic molecules* (Wiley, New York, 1970).
- 7 D. Georgescauld, J.P. Desmasez, R. Lapouyade, A. Babeau, H. Richard and M. Winnik, *Photochem. Photobiol.* 31 (1980) 539.
- 8 R.L. Melnick, H.C. Haspel, M. Goldenberg, L.M. Greenbaum and S. Weinstein, *Biophys. J.* 34 (1981) 499.
- 9 M. Vauhkonen, M. Sassaroli, P. Somerharju and J. Eisinger, *Biophys. J.* 57 (1990) 291.
- 10 S.M. Gruner, P.R. Cullis, M.J. Hope and C.P.S. Tilcock, *Annu. Rev. Biophys. Biophys. Chem.* 14 (1985) 211.
- 11 S. Das and R.P. Rand, *Biochemistry* 25 (1986) 2882.
- 12 K.H. Cheng, *Chem. Phys. Lipids* 51 (1989) 137.
- 13 L.T. Boni and S.W. Hui, *Biochim. Biophys. Acta* 731 (1983) 177.
- 14 K.M. Patel, J.D. Morrisett and J.T. Sparrow, *J. Lipid Res.* 20 (1979) 674.
- 15 J. Eisinger and J. Flores, *Biophys. J.* 48 (1985) 77.
- 16 J.R. Lakowicz and B.P. Maliwal, *Biophys. Chem.* 21 (1985) 61.
- 17 P.L. Chong and T.E. Thompson, *Biophys. J.* 47 (1985) 613.
- 18 K.H. Cheng, *Biophys. J.* 55 (1989) 1025.